NACA RM A51K05

NACA

RESEARCH MEMORANDUM

OBSERVATIONS OF UNSTEADY FLOW PHENOMENA FOR AN INCLINED BODY FITTED WITH STABILIZING FINS

By Merrill H. Mead

Ames Aeronautical Laboratory,
Moffett Field, Calif.

NATIONAL ADVISORY COMMITTEE
FOR AERONAUTICS

WASHINGTON

January 17, 1952
Declassified April 8, 1957

NATIONAL ADVISORY COMMITTEE FOR AERONAUTICS

RESEARCH MEMORANDUM

OBSERVATIONS OF UNSTEADY FLOW PHENOMENA FOR AN INCLINED BODY FITTED WITH STABILIZING FINS

By Merrill H. Mead

SUMMARY

The variations with Mach number and angle of attack of the dynamic rolling-moment characteristics of a slender body of revolution in combination with a cruciform tail have been investigated in the Ames 6- by 6-foot supersonic wind tunnel. Oscillograph records of the instantaneous rolling moment of the model were obtained for Mach numbers of 0.90, 1.20, 1.40, 1.53, 1.60, and 1.70 at a constant free-stream Reynolds number of 0.84×10^6 based on maximum body diameter. The model was tested at angles of attack of from 0° to 27°. Visual flow studies were made of the cross-flow field in the region of the tail at Mach numbers of 1.2, 1.4, and 1.7 at the same free-stream Reynolds number. The "vapor screen technique" was used for the flow studies, and representative photographs of the flow field, obtained from these studies, are presented.

Analysis of the data indicated that the model began to experience oscillating rolling moments at about 10° angle of attack at each Mach number for which tests were made, and that the variations with angle of attack of the rolling moments were, in general, similar for each Mach number. Throughout most of the angle-of-attack range, an increase in Mach number was accompanied by a decrease in the magnitudes of the oscillating rolling moments.

INTRODUCTION

Current emphasis on the design of missiles and supersonic aircraft has occasioned a renewed interest in the aerodynamic characteristics of bodies of revolution. Of particular significance has become the nature of the flow field behind inclined bodies of revolution. Although it has long been recognized that this flow field differs markedly from the potential flow considered by Munk (reference 1), the presence of vortex

flow in the lee of such bodies has only recently manifested itself as a serious problem to the missile and aircraft designer. A recent paper by Allen and Perkins (reference 2) discusses an approximate method for estimating the forces and moments on inclined bodies of revolution in which the effects of viscosity are taken into consideration. In this paper, the development with distance along the body of the viscous cross-flow field behind the inclined body was related to the development with time of the flow field behind a circular cylinder set in motion impulsively from rest. It was shown that, for moderate angles of attack, the body flow field contained a symmetrically disposed pair of vortices which increased in strength, and separated farther from the body, with distance downstream. These observations, as well as the results of circumferential pressure distributions measured at several stations along the body, were in qualitative agreement with the results of an experimental investigation made by Schwabe in reference 3 on the development of the flow field behind a circular cylinder impulsively set in motion from rest. Further, it was shown in reference 2 that as the body angle of attack increased from moderate to large values, the strength of the vortices increased more rapidly with distance downstream. In addition, it was noted that, a short distance aft of the ogival nose section, this unstable symmetrical-pair configuration began to discharge as a street of alternate vortices characteristic of that known to exist behind a circular cylinder in two-dimensional flow. Of particular interest to the present investigation was the less familiar phenomenon, observed during the tests reported in reference 2, of aperiodic reversals of the vortex-street configuration. At one instant, the street of vortices was so distributed that the vortex closest to the body would appear at the left side of the body, and at the next instant the entire street of vortices would change sides, the first vortex from the body then appearing on the right. The reversing action was apparently of an entirely aperiodic nature, no regularity having been observed throughout the tests. No explanation for these reversals was attempted, but it was suggested in reference 2 that, for aircraft and missile designs which would incorporate long slender bodies of revolution with tail surfaces at the aft end and which would be expected to maneuver at large angles of attack, the discharge of a vortex street and the development of such a reversing action should manifest itself as an erratic rolling tendency as a result of the aperiodic asymmetry of forces on the tail surfaces.

To investigate the nature of the rolling moments experienced by one such configuration, a body-tail combination has been tested in the Ames 6- by 6-foot supersonic wind tunnel at Mach numbers ranging from 0.9 to 1.7. The tests were performed to provide information on the effects of angle of attack and Mach number on the magnitude of the instantaneous rolling moments induced on a typical missile configuration.

TEST METHODS AND APPARATUS

Wind Tunnel

The test was performed in the Ames 6- by 6-foot supersonic wind tunnel which is a closed-return, variable-pressure supersonic wind tunnel in which the Mach number can be varied continuously from 1.15 to 1.9 while the tunnel is in operation and which also can be operated at subsonic Mach numbers of 0.6 to 0.93. The wind tunnel and its stream characteristics are described in detail in reference 4. The model was supported in the wind tunnel on a conventional sting-type support and was pitched in the horizontal plane.

Model

The model used in the present investigation consisted of a combination of body and cruciform tail typical of one type of missile design currently being studied. The geometric characteristics of the model are given in figure 1. Of hollow construction, the cylindrical portion of the body was of steel, and the ogival nose of aluminum. Steel tail fins, of triangular plan form and aspect ratio 4 with a double-wedge section 3-percent thick, were mounted at the aft end of the body in the vertical and horizontal planes.

Instrumentation for Force Tests

The model was mounted in the wind tunnel on a short sting extension which was fitted to the end of the conventional support sting. Strain gages were located on the sting extension at two longitudinal positions, one forward and one rearward. The model and sting extension were restrained in roll by a torsion-type spring located inside the sting. The strain gages on the sting extension were mounted in such a manner that changes in their resistance would provide an indication of the lateral (yawing) motions of the model (fig. 1), while changes in resistance of the rolling-moment gages, mounted on the torsion spring, measured the rolling moments. For obtaining measurements of the oscillating loads, a 2,000 cycle-per-second carrier system was used. This system employs an amplitude-stabilized electronic oscillator to provide input voltages to the strain gages. The outputs of the gages are passed through an electronic band-pass amplifier, the flat pass band of which is 800 cps in width centered about the carrier frequency. The output of the amplifier is demodulated, producing signals the amplitude and frequency of which reproduce the variation of loads applied to the strain-gage transducer

with a maximum error of 3 percent of full-scale deflection. These output signals are recorded with a photographic oscillograph using D'Arsonval elements which reproduce the amplitudes of the signals with a flat response from 0 to 160 cps, and which accurately indicate signal frequencies from 0 to 500 cps.

Static calibrations were made of the strain gages periodically throughout the test period by the standard method of applying known loads to the model and recording the resulting deflections on the oscillograph. It was found to be impossible, however, to calibrate the gages on the sting extension with the required accuracy. Therefore, the recorded outputs of these gages are included in the report to represent only the frequency of the lateral oscillations of the model.

Visual Flow Studies

In order to investigate the cross-flow field around the body in an attempt to correlate the development of the body vortices with the recorded variations in rolling moment, use was made of a flow visualization technique, described in reference 2, which has been termed the "vapor-screen method." In this technique, a small amount of water is introduced into the wind tunnel which results in the condensation of a fine fog at the test section. A narrow plane of intense light, created by a high-pressure mercury-vapor lamp, is made to shine across the test section in a plane essentially perpendicular to the air stream. In the regions of undisturbed flow, the effect of the plane of light through the fog is to produce a uniformly lighted screen of fog particles. In the region of the disturbed flow around the model, however, the fog is inhomogeneous and the flow disturbances appear on the screen as areas of varying brightness. In the present test, a 16 mm camera, mounted on the support sting 20 inches downstream of the tail of the model, was used to photograph the cross-flow field as seen in the vapor screen. Moving pictures were made with the light screen intersecting the model at a position corresponding to the location of the tail on the body. The model was tested with the tail removed for the vapor-screen studies, in order that the camera have an unobstructed view of the body flow field in the vapor screen.

Test Procedure

The test was conducted in two phases: the force tests on the body-tail combination first; and the visual flow studies, made with the body alone, later. During the first phase of the test program, in which the measurements were made of the instantaneous rolling moments, the model

was tested at Mach numbers of 0.9, 1.2, 1.4, 1.53, 1.6, and 1.7 at a free-stream Reynolds number of 0.84×10^6 based on maximum body diameter. The dynamic pressure increased with Mach number from 510 pounds per square foot at 1.2 to 590 pounds per square foot at 1.6. Due to lower tunnel temperatures, the dynamic pressure was 550 pounds per square foot at 1.7 Mach number. The majority of the tests were performed in the angle-of-attack range from 10° to 27° since it was observed that there were no oscillating rolling moments of significant magnitude registered on the instruments from 0° to 10° angle of attack. Some data were obtained at 0°, however, to determine the level of transient vibrations recorded by the oscillograph. For all Mach numbers, with the exception of 0.9, data were recorded at 1° increments in angle of attack throughout the 10° to 27° range. The maximum angle was limited to 20° in the 0.9 Mach number case because of excessive model vibrations.[1]

For the visual flow study tests, the tail was removed from the model and replaced by a cylindrical shell which was faired in smoothly with the forward portion of the body. With the wind tunnel operating at the same free-stream Reynolds number as in the force tests, the model was tested at Mach numbers of 1.2, 1.4, and 1.7. At each Mach number, the model angle of attack was varied from 10° to 27° while the camera recorded the flow patterns formed in the vapor screen.[2] The photographs included in this report are enlargements of frames from these films.

RESULTS

A wide interest has recently been shown in the problem of erratic rolling moments induced on inclined bodies of revolution fitted with tail fins by the separated flow about the body. In view of the fact that little information on this subject has been published to date, the results of the present investigation are made available to the reader, even though they are in a very preliminary form and indicate the need for further study and instrumentation development. The reader is cautioned to bear in mind that the results are, for the most part, qualitative.

---

[1] Severe lateral vibrations of the model were observed during a previous investigation in which the body with the tail removed was tested under similar conditions. It is believed, therefore, that the vibrations observed at the subsonic Mach number during the present investigation were not the result of fluctuating forces on the tail.

[2] Several attempts to obtain vapor-screen pictures of the flow field at 0.9 Mach number were unsuccessful because of difficulties encountered in maintaining the proper fog density in the wind tunnel.

Reproductions of typical oscillograph records for three Mach numbers and a series of angles of attack are presented in figure 2. The upper trace in each record represents the rolling moment, and the two lower traces are indications of the lateral motion of the model. In the latter case, the output of the most rearward strain gage is represented on the oscillograph records by the trace having the larger amplitudes of the two. It should be pointed out that the sensitivities of the two lateral-motion gages were much greater than that for the rolling-moment gage; hence, comparisons of amplitudes of the rolling-moment and yawing-moment traces have no significance. It should also be stated that the vertical positions of the rolling-moment traces on the oscillograph records are not indications of the static rolling moments imposed on the model. No attempt was made during the present tests to measure static rolling moments. The changes of the paper speed control on the oscillograph, which appear as different spacings of the timing lines for different Mach numbers, did not vary the response characteristics of the instrument. With the exception of those for an angle of attack of 0°, each record is accompanied by a photograph of the cross-flow field at the tail of the body, obtained by the vapor-screen technique. To facilitate interpretation of these photographs, two typical vapor-screen pictures, for an angle of attack of 18° and Mach numbers of 1.2 and 1.7, are presented in figure 3 accompanied by diagrammatic sketches of the cross-flow fields. Variations with angle of attack of the indicated levels of instantaneous rolling moment for Mach numbers of 0.9, 1.2, 1.4, 1.53, 1.6, and 1.7 are shown in figure 4. In obtaining the values for the ordinates of these curves, two horizontal linear envelopes were drawn which bounded the majority of the waves for each of the traces of instantaneous rolling moment obtained from the oscillograph records. The "indicated level of instantaneous rolling moment" was taken as one-half of the double amplitude defined by the envelopes. In this plot the rolling moments are presented in coefficient form, based on tail span and exposed area of the horizontal tail surfaces, and the magnitudes of the curves represent a measure of the recorded moment fluctuations uncorrected for mechanical amplification. The significance of the mechanical amplification is discussed in the next section.

DISCUSSION

Before discussing the results of the investigation in any detail, it is advisable to point out a few of the factors involved in obtaining the data in order that the reader may be better equipped to interpret and evaluate them. The model, as mounted in the wind tunnel, constituted a spring and mass system vibrating torsionally - the model representing the mass, and the rolling-moment gage representing the spring. The natural frequency of torsional vibration for the system was determined experimentally to be between 65 and 70 cps. It was observed that this was also

the predominant frequency of the rolling-moment variations recorded during the tests. It does not necessarily follow, however, that this is an indication of the forcing frequency for the system, that is, the frequency at which the model was receiving rolling impulses. Since the model was essentially spring mounted and free to oscillate, the natural frequency might be expected to predominate over a number of possible input functions. For example, a very low forcing frequency should result in model oscillations at the lower frequency with the natural frequency superimposed as a transient, while aperiodic impulses might be represented by oscillations at the natural frequency with modulations appearing in the amplitudes.

Studies of all of the records obtained during the tests, including those presented in figure 2, indicate a completely random variation of rolling-moment amplitude with time. There were very few instances of sustained oscillation at a constant amplitude such as would be expected for the condition of a sinusoidal forcing function of constant amplitude. There were, on the other hand, few instances of a modulated amplitude which would be associated with aperiodic disturbances. Furthermore, since the amplitudes of the forcing functions were subject to any mechanical amplification present in the vibrating system, and since this amplification cannot be determined without knowledge of the frequency of the forcing function or, for aperiodic disturbances, the wave shape and rise time, it was not possible to determine values of the forcing-function amplitudes from the results of the present investigation.

It is clear from the above considerations, therefore, that, because of the limitations of the instrumentation used, the results of the present tests provide little information as to the nature of the disturbing forces imposed on the model in roll. However, the rolling-moment records obtained during the tests are considered significant representations of the variations of the rolling moments imparted to the model by these forces. Of particular interest was the marked effects of Mach number and angle of attack on the amplitudes of the rolling moments apparent from an inspection of the data. In order to present these effects in a comparison plot, the average level of the rolling-moment amplitudes for each angle of attack at each Mach number have been plotted in coefficient form in figure 4. It should be emphasized that the ordinates of these curves represent the level of oscillations and not the maximum single-wave peaks.

Dynamic Rolling Moments

The dynamic rolling moments experienced by the model during the present tests, records of which are reproduced in figure 2, showed a significant effect of Mach number. From an examination of figure 2, it can be seen that for each angle of attack the amplitude levels of the

oscillating rolling moments were of greatest magnitude at 1.2 Mach number, generally less at $M = 1.4$, and relatively small at $M = 1.7$. In general, within the range of Mach numbers from 1.2 to 1.7, this trend was consistent throughout the tests, rolling-moment amplitude levels decreasing with increasing Mach number. The predominant frequency of oscillation of the model in roll is shown in the records of figure 2 to have been between 65 and 70 cps, which was the natural frequency of the system in torsional vibration, and the significance of which has been discussed previously. It will also be noted from the records of figure 2 that the frequency of lateral motion of the model was approximately 13 cps, which was determined experimentally to be the natural frequency of lateral vibration for the system, and that this frequency is not apparent in any of the typical rolling-moment traces presented, nor was it in any of the rolling-moment data obtained throughout the tests. Thus apparently no interaction existed between the lateral motion of the model and the measured rolling moments. The amplitude levels of the oscillating rolling-moment traces of figure 2, as well as those for Mach numbers for which the records were not included in this figure, are plotted in figure 4 in coefficient form against angle of attack. The influence of Mach number on the magnitudes of the rolling-moment amplitudes is plainly evident in this figure. It can be seen in this figure that, as stated previously, the magnitudes of the rolling moments, in general, decreased with increasing Mach number. It is also apparent that the variations of the amplitude levels with angle of attack were fairly consistent for all supersonic Mach numbers at which tests were made. In each case, peak levels were recorded at between 16° and 18° angle of attack, following which the amplitudes fell off sharply, then increased again to a second peak, lower than the first, at approximately 23°.

Visual Flow Studies

The vapor-screen technique, which has been used in the present investigation for the visualization of the body flow field, is a relatively recent development in the field of visual flow studies and refinements have yet to be made in its application. Within its limitations, however, the use of the technique has proven a valuable aid in understanding the origin of the irregularities in the forces and moments obtained from wind-tunnel tests. It was intended that the results of the vapor-screen studies made in conjunction with the present investigation would make known the locations of the body vortices with respect to the tail, any irregularities in the vortex configurations, and, through the projection of the motion pictures, any dynamic instabilities within the flow field such as were observed during the tests of reference 2. It should be pointed out, with regard to the motion pictures, that, due to the limitations of the photographic equipment used, it was necessary

to operate the camera at the relatively slow speed of 4 frames per second during the tests in order to obtain the proper exposure. There exists, therefore, the possibility that disturbances of a very short duration in the vortex pattern could have been missed by the camera. It will also be noted from figure 2 that, in the photographs for 1.2 Mach number, the vortices generally appear as light areas, while those at Mach number 1.7 are dark. At 1.4 Mach number, for angles of attack above 16°, the vortices are almost obscured by a dark area which apparently outlines the disturbance region, but above which there appears a very light area. No explanation has been found for these phenomena, but they are believed to have had no relation to the rolling-moment oscillations.

A study of the motion pictures of the cross-flow field, obtained by the vapor-screen method, representative prints from which are reproduced in figure 2, indicated that the flow field did not develop the expected vortex street in cross-flow planes within the range of angles of attack tested.[3] Conditions of instability within the flow field were observed, however, which, it is believed, may have produced the fluctuation of forces at the tail resulting in the measured rolling moments, even before the vortices had begun shedding from the body. At a Mach number of 1.2, for angles of attack below 10°, the flow field contained a symmetrically disposed pair of vortices apparently stable and located close to the body. Above $\alpha = 10°$, however, the vortex pattern rapidly became unsymmetrical, the left vortex leaving the body, rising above, and curling around the right vortex. At 18° angle of attack, an intermittent lateral motion of the right (lower) vortex was observed. The vortex appeared to move abruptly to the right, then to the left, aperiodically. The vortices did not reverse positions, however, as was observed in the tests of reference 2. This phenomenon was less apparent at 20° and disappeared at 22°. However, at $\alpha = 24°$, the condition again appeared, and was visible through $\alpha = 26°$. Referring to the curves of figure 4, it is evident that the appearance of this motion in the flow field coincided closely with the angles at which maximum rolling moments were measured for 1.2 Mach number. The photographs accompanying the oscillograph records for 1.2 Mach number in figure 2 show the relative positions of the vortices at the various angles of attack, demonstrating the asymmetry of the pattern, but obviously cannot show the dynamic instabilities revealed by the motion pictures.

---

[3] This observation pertains only to the results of the tests herein reported. Discussions with the authors of reference 2 have indicated that for a model with a cylindrical afterbody, the nose shape may have a significant influence on the angle-of-attack range in which a vortex street is discharged.

At 1.4 Mach number, for angles of attack below 10°, the vortex pattern was much the same as for 1.2 Mach number at the same angles. However, as the angle of attack was increased above 10°, the vortex pattern became unsymmetrical much less rapidly than at the lower Mach number. Both vortices, which had appeared as round dots, were observed to elongate vertically at very nearly the same rate until, at 16°, the configuration was only slightly asymmetrical, but, in general, larger than at 1.2 Mach number. As was mentioned previously, for angles of attack above 16°, the photographs contained a dark area which appeared to outline the disturbance region, and the individual vortices were not visible. It was observed, however, that the outline itself became more asymmetrical as the angle of attack was increased to 27°, and presumably this was associated with the increasing unbalance of the vortices within. No lateral motion of the vortices was visible at this Mach number, but it is probable that if this condition had existed it would have been obscured in the dark regions of the film.

The motion pictures for 1.7 Mach number provide some explanation for the very low rolling-moment amplitudes measured at this Mach number during the force tests. It was observed that in this case the vortex configuration remained stable and symmetrical up through nearly 20°, and that even at $\alpha = 27^{\circ}$ the asymmetry was not nearly as pronounced as that for 1.2 Mach number and corresponding angles of attack. Further, it was observed that although the flow field was plainly visible in the motion pictures throughout the angle-of-attack range, no fluctuating lateral motions of the vortices appeared at any time. In the photographs of figures 2(f), 2(g), and 2(h) for 1.7 Mach number, the shock wave, which is faintly visible on either side of the vortex pattern, is a result of the cross flow around the body having exceeded the critical Mach number, about 0.4 for circular cylinders. (See reference 5.) At an angle of attack corresponding to a cross-flow Mach number of 0.4, the shock wave emanates from the body; however, as the cross-flow Mach number is increased (increasing angle of attack) the shock wave moves up on the wake, as seen in the photographs. Although the critical cross-flow Mach number was exceeded for every free-stream Mach number at which the model was tested during this investigation, the shock wave was visible in the vapor-screen pictures only in these three instances. What influence the shock wave had on the vortex configurations or on the resulting rolling moments is not known.

CONCLUDING REMARKS

Although the results of the present investigation are of a preliminary nature only, and the instrumentation has not been sufficiently developed to provide quantitative data, the information obtained from these tests does substantiate one salient fact: that for the particular body-tail combination tested, there was a marked effect of Mach

number on the magnitudes of the oscillating rolling moments of the model at angles of attack. The magnitudes of the oscillations decreased consistently with increasing Mach number, within the Mach number range tested. Also considered significant was the consistency with which the variation of rolling-moment amplitudes with angle of attack followed similar trends at supersonic Mach numbers.

Ames Aeronautical Laboratory,
National Advisory Committee for Aeronautics,
Moffett Field, Calif.

REFERENCES

1. Munk, Max M.: The Aerodynamic Forces on Airship Hulls. NACA Rep. 184, 1924.

2. Allen, H. Julian, and Perkins, Edward W.: Characteristics of Flow Over Inclined Bodies of Revolution. NACA RM A50L07, 1951.

3. Schwabe, M.: Pressure Distribution in Nonuniform Two-Dimensional Flow. NACA TM 1039, 1943.

4. Frick, Charles W., and Olson, Robert N.: Flow Studies in the Asymmetric Adjustable Nozzle of the Ames 6- by 6-foot Supersonic Wind Tunnel. NACA RM A9E24, 1949.

5. Allen, H. Julian: Estimation of the Forces and Moments Acting on Inclined Bodies of Revolution. NACA RM A9I26, 1949.

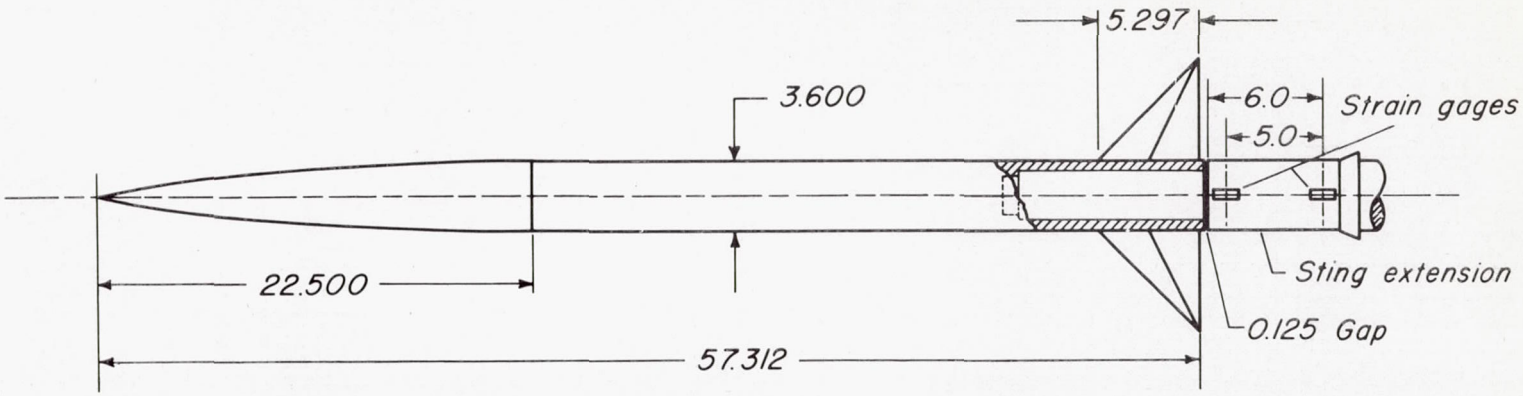

Side view of model with tail in place

Geometric characteristics

Body fineness ratio: 15.9
Tail aspect ratio: 4.0
Nose shape: ogive

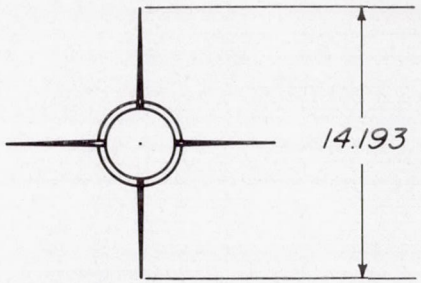

Front view

All dimensions in inches

Figure 1.- Diagrammatic sketch of model.

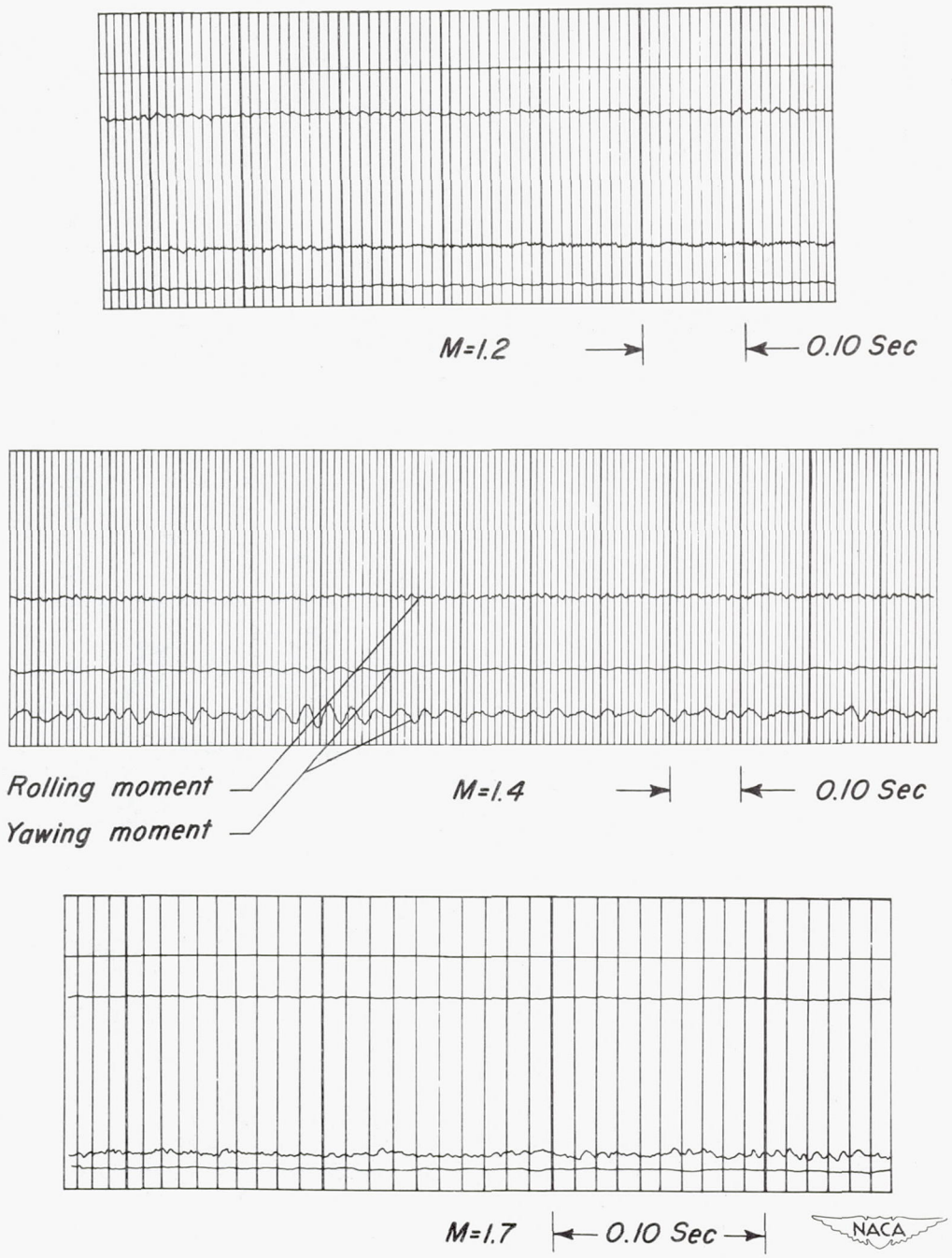

(a) $\alpha = 0°$

Figure 2.- Comparison of instantaneous rolling moments at three Mach numbers for various angles of attack.

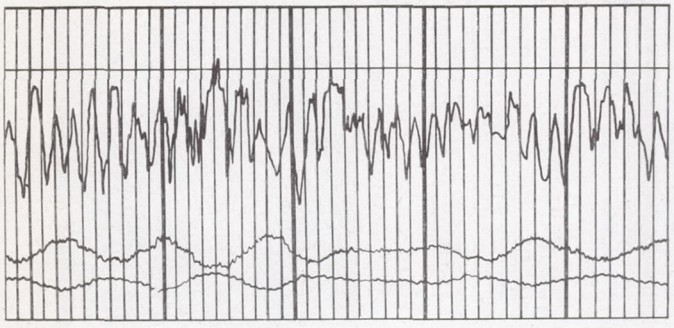

M=1.2

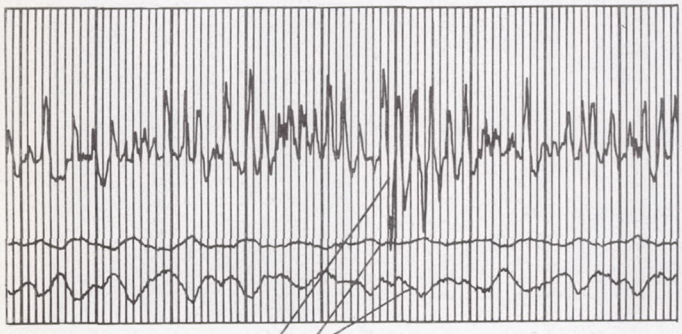

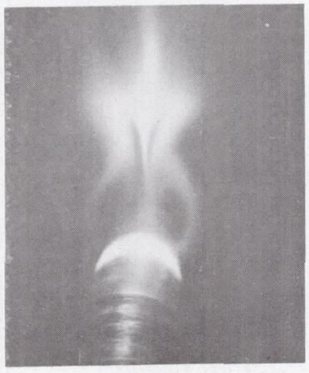

Rolling moment

Yawing moment

M=1.4

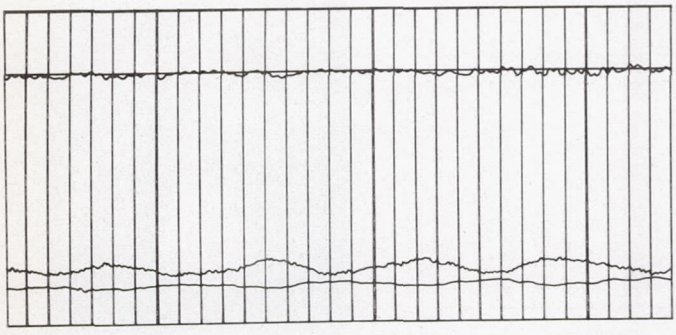

M=1.7

(b) α=16°

Figure 2.- Continued.

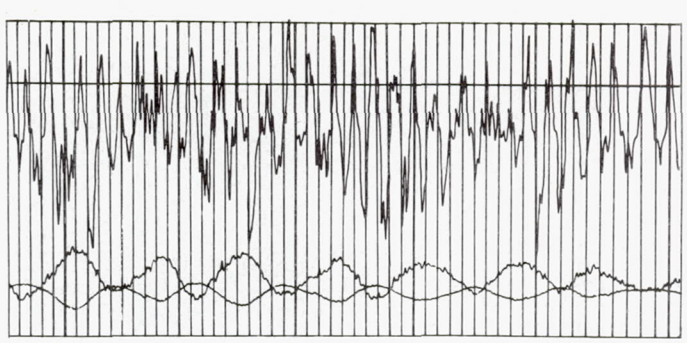

M=1.2

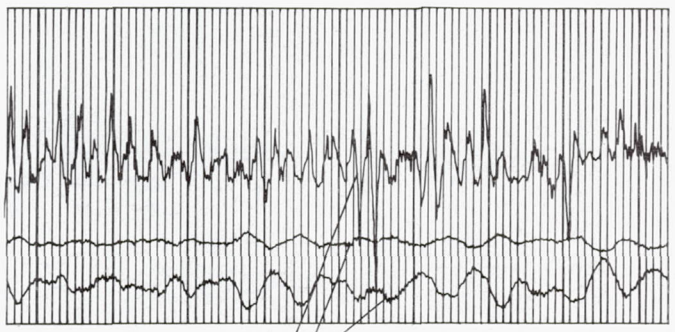

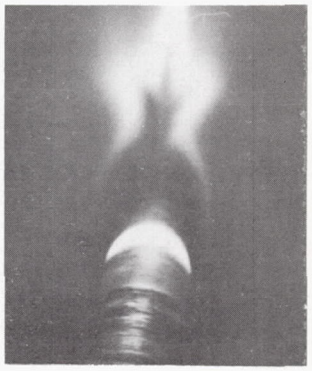

Rolling moment

Yawing moment

M=1.4

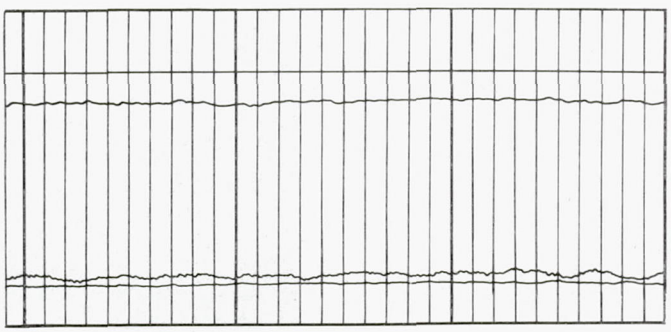

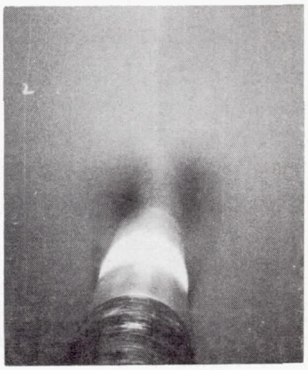

M=1.7

(c) $\alpha = 18°$

Figure 2. – Continued.

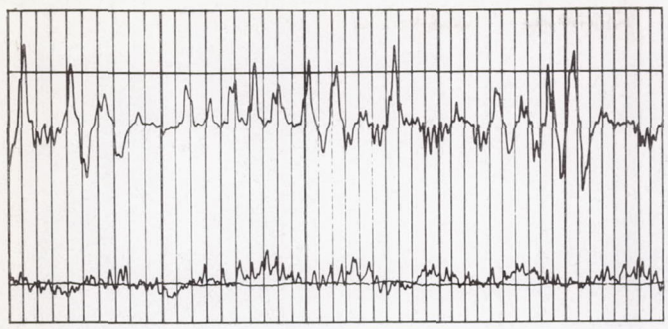

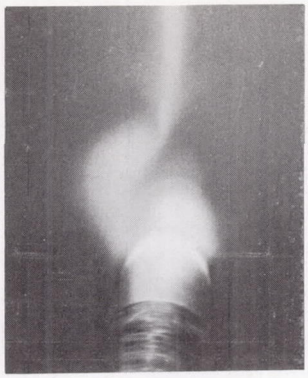

M=1.2

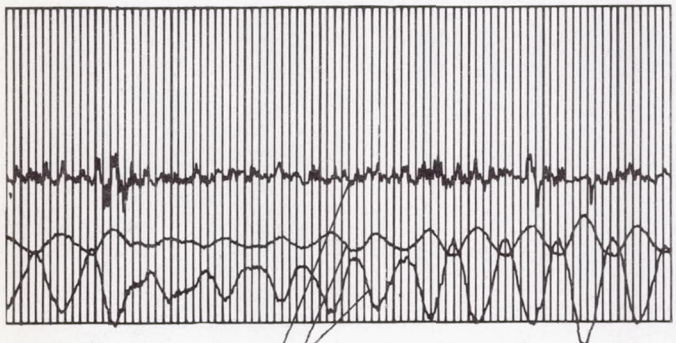

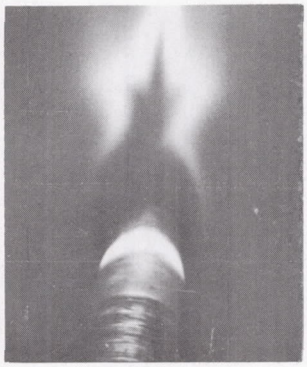

Rolling moment

Yawing moment

M=1.4

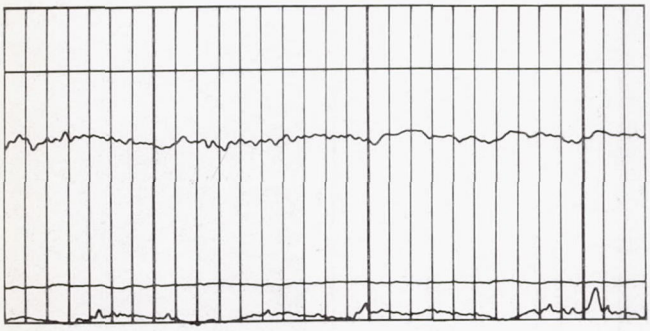

M=1.7

(d) $\alpha = 20°$

Figure 2.– Continued.

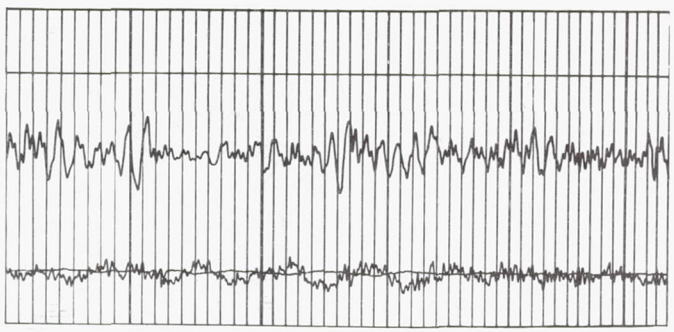

M=1.2

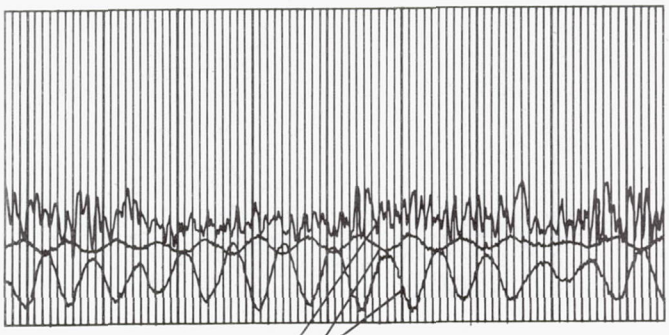

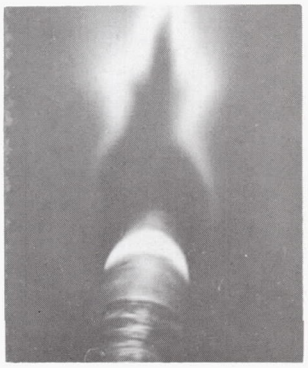

Rolling moment

Yawing moment

M=1.4

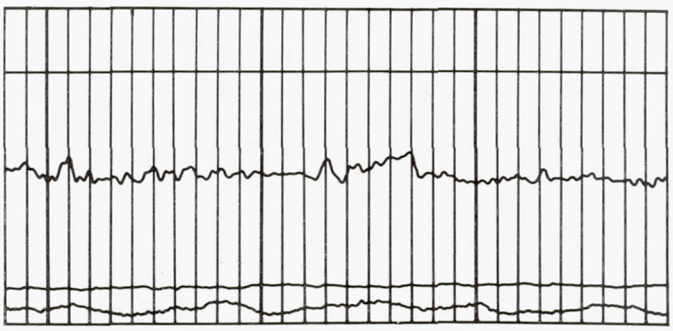

M=1.7

(e) $\alpha=22°$

Figure 2.- Continued.

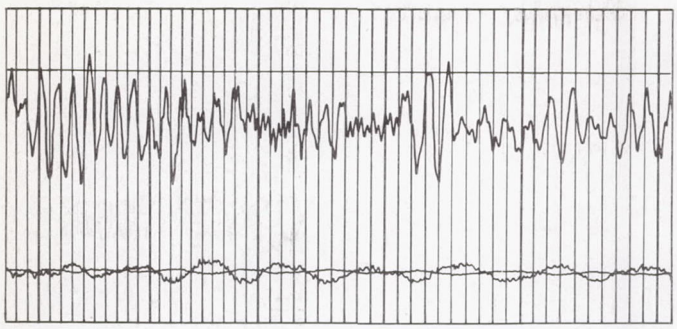

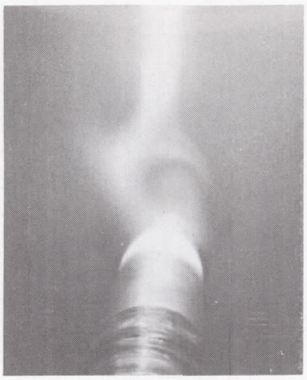

M=1.2

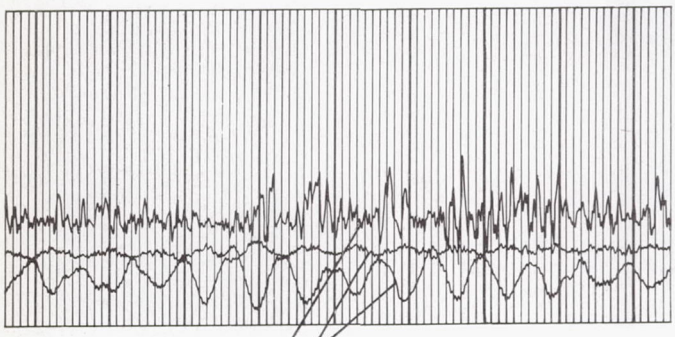

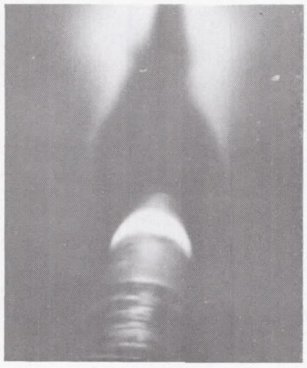

Rolling moment

Yawing moment

M=1.4

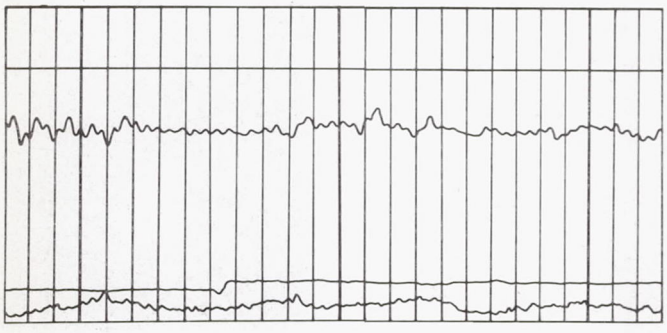

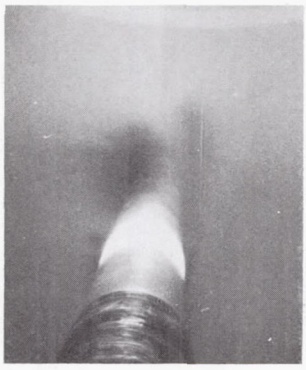

M=1.7

(f) $\alpha = 24°$

Figure 2. – Continued.

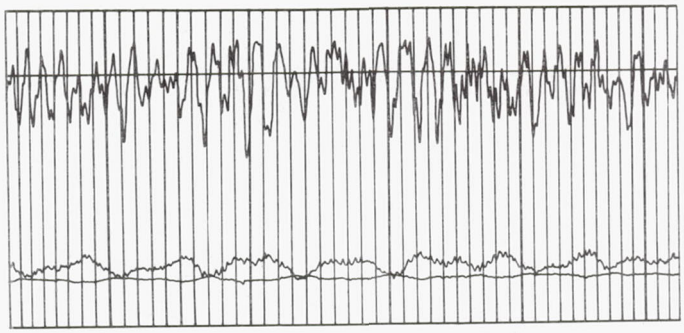

M=1.2

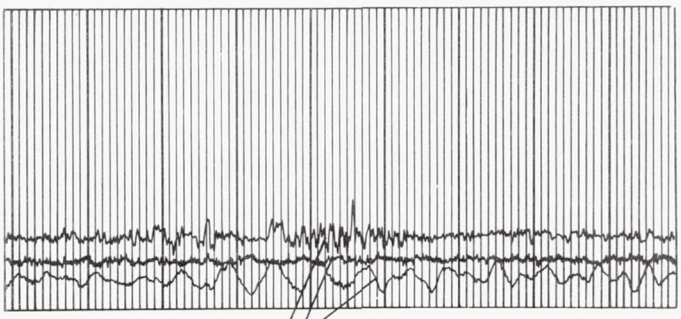

Rolling moment

Yawing moment

M=1.4

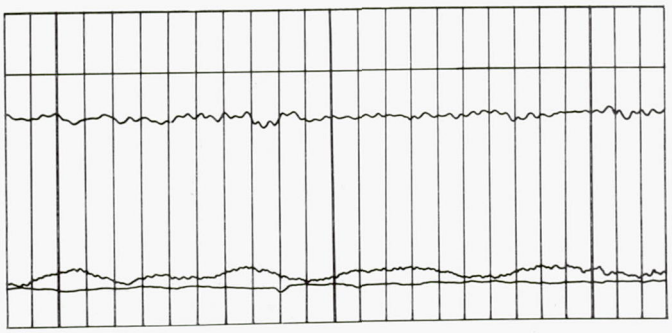

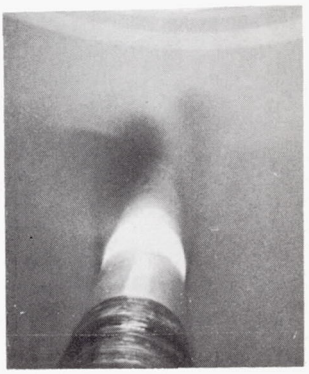

M=1.7

(g) $\alpha=26°$

Figure 2.- Continued.

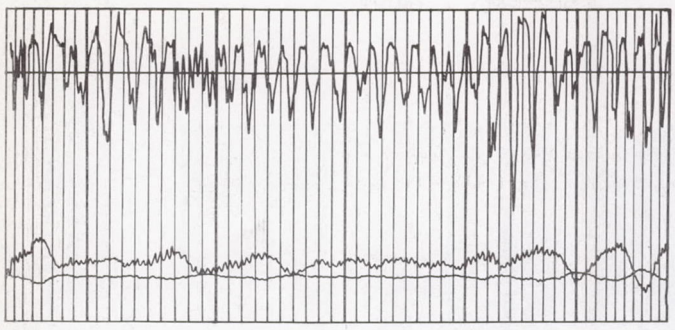

M=1.2

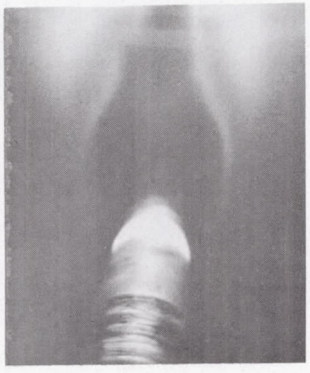

Rolling moment

Yawing moment

M=1.4

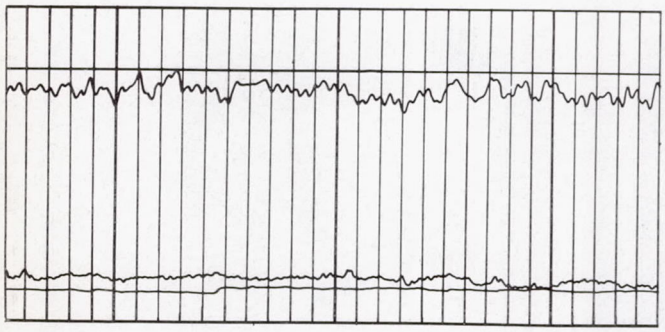

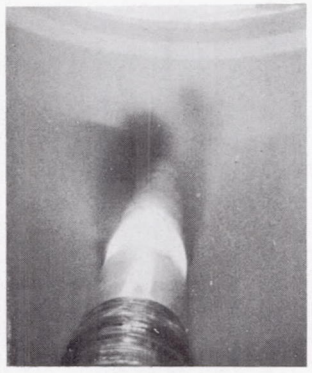

M=1.7

(h) $\alpha=27°$

Figure 2.- Concluded.

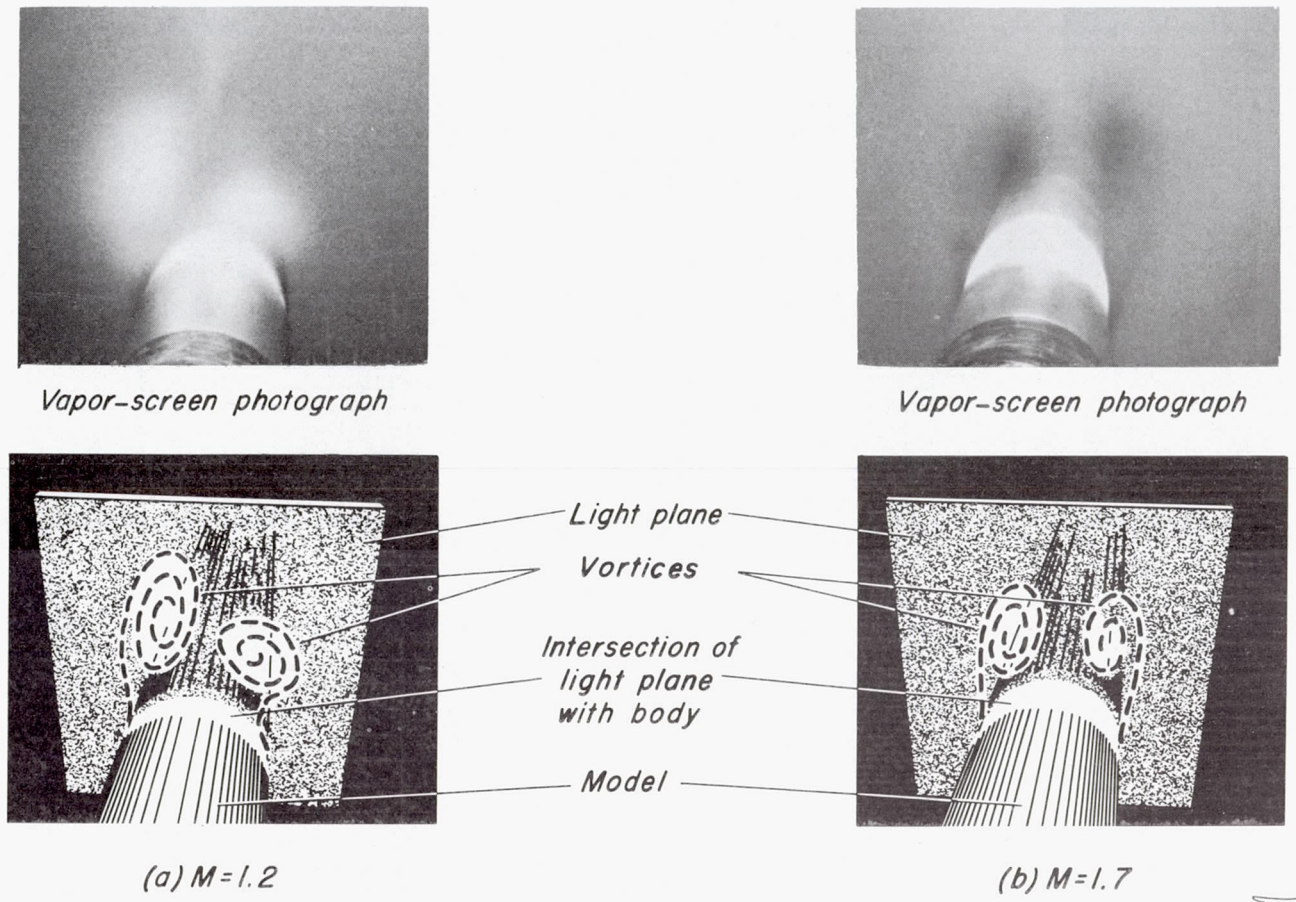

Figure 3.- Diagrammatic sketch of cross-flow field as represented by vapor-screen photographs for 18° angle of attack at two Mach numbers.

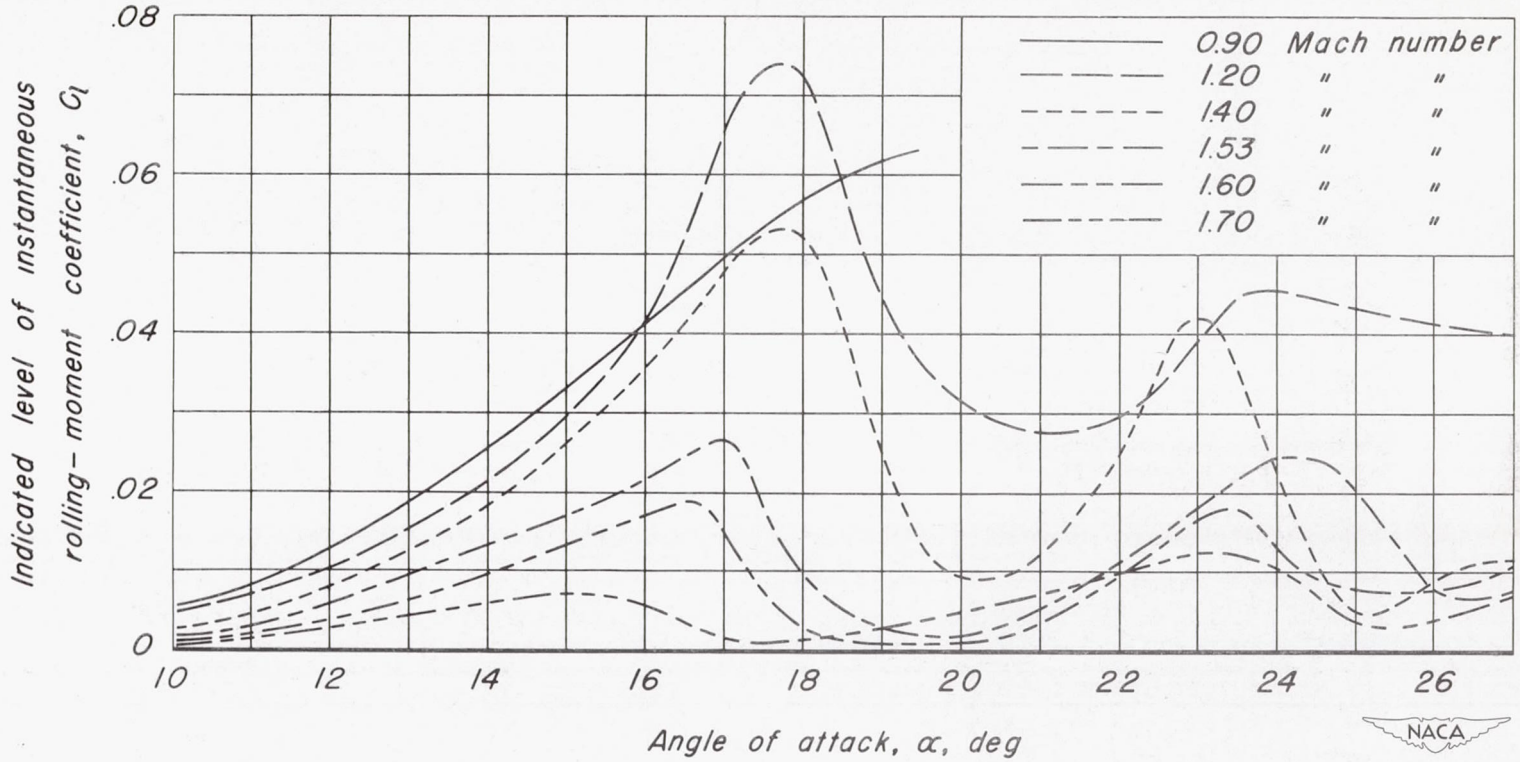

Figure 4.— Variation of indicated level of instantaneous rolling-moment coefficient with angle of attack for six Mach numbers.